

Multiscale Mechanics of Graphene Fracture under Thermal Gradients using Empirical and Machine-Learned Interatomic Forcefields

Hanfeng Zhai¹ Jingjie Yeo^{1, 2}

¹Sibley School of Mechanical and Aerospace Engineering, Cornell University

²Materials Science and Engineering, Cornell University

Key Highlights

- Nonequilibrium molecular dynamics were employed to study graphene fracture under temperature gradients with fixed strain rate, where the effect of initial defect sizes, temperature differences, and potential fields are investigated.
- Different empirical potential fields, including optimized Tersoff, REBO, AIREBO, and AIREBO-M are employed in the NEMD simulations.
- Quantized fracture mechanics are adopted to verify the computations from NEMD.
- A comparative study of empirical MD potentials with state-of-the-art *ab initio*-based machine learning potentials is also presented, where the limitations and the fracture characterizations are elaborated.
- The overall goal is: (1) identify the effect of different potential models, characterize the mechanics from simulations corresponding to the mathematical models; (2) unveil the mechanism under the thermal gradient fractures independent of potential fields.

Modeling & Simulations

A three-dimensional simulation box with X and Y directional lengths of 50 nm, and Z directional height of 6 nm were set with full periodic boundary conditions on each surface, as shown in Figure 1. The X direction is the armchair direction and Y is the zigzag direction. A thermal gradient was applied in the Y direction, where the bottom is the heat source and the upper side is the heat sink. A defect is set in the center of the graphene layer, of different lengths to account for the sizing effects of precrack. A strain rate of 10^9 s^{-1} is applied in the X direction for crack propagation.

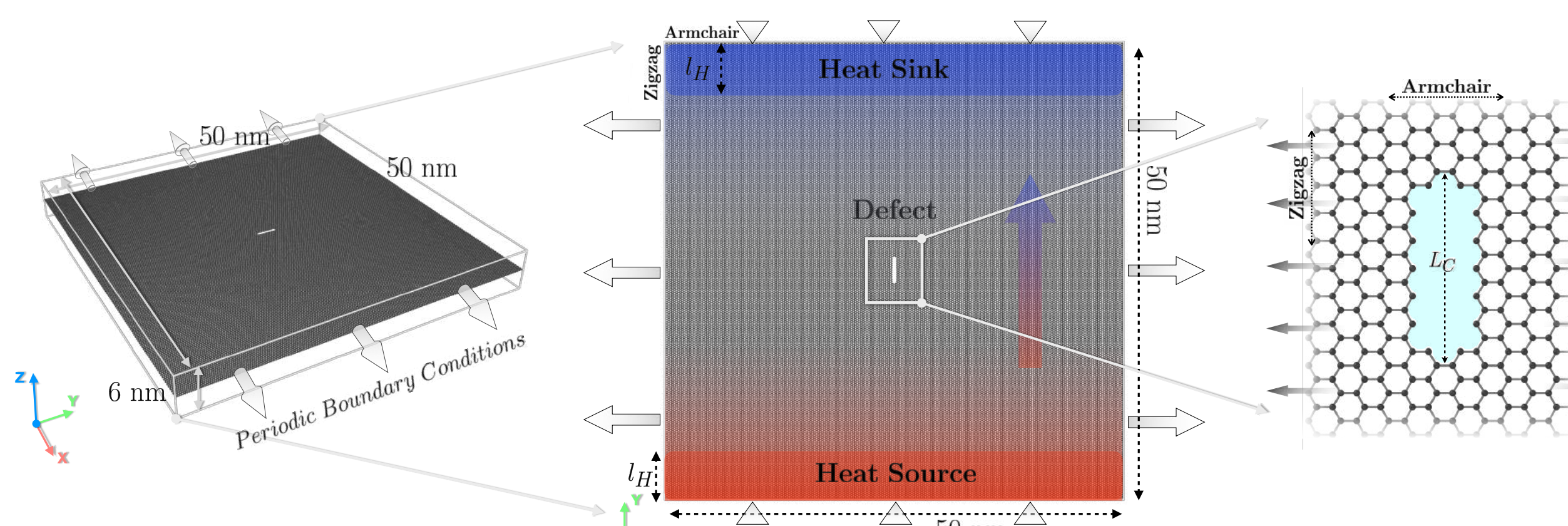


Figure 1. Schematic illustration of the simulation setup.

Deep Learning Potential Fields

Machine learning potentials (MLPs) based on first principle calculations. The atomic configurations in first principles, i.e., DFT, AIMD, include locations, radius, etc., are transformed into symmetry functions based on the formulation by Behler and Parrinello [1]:

$$G_i^R = \sum_{j \neq i}^{\text{all}} \mathcal{F}_R(r_{ij}) f_C(r_{ij}), \quad G_i^A = \sum_{j,k \neq i}^{\text{all}} \mathcal{F}_A(r_{ij}, r_{ik}, r_{jk}) f_C(r_{ij}) f_C(r_{ik}) f_C(r_{jk}) \quad (1)$$

The output energies are approximated via a neural network of L layers. The eventually learned energy is the summation of the atomic energies, $E = \sum_i E_i$, where

$$E_i = (K_L \circ \sigma_L \circ \dots \circ K_1 \circ \sigma_1 \circ K_0) [G_i^R, G_i^A] \quad (2)$$

Four different such MLPs, dropout uncertainty neural networks with different dropout rates [8], and moment tensor-based machine learning interatomic potential [4], are adopted to benchmark the molecular simulations.

Multiscale Mechanics Theories

- Molecular dynamics.** Both the REBO [2] and Tersoff [3] models have similar energy fields following the form

$$E_{ij}^{\text{REBO}} \setminus / E_{ij}^{\text{Tersoff}} = \sum_{j \neq i} f_c^{\text{REBO}}(r_{ij}) \setminus / f_c^{\text{Tersoff}}(r_{ij}) [V_R(r_{ij}) + b_{ij} V_{ij}^A] \quad (3)$$

and other REBO-based potentials, i.e., AIREBO [7], AIREBO-M [5] takes the general form of

$$E^{\text{AIREBO-M}} = E^{\text{REBO}} + E^{\text{Morse}} \setminus / E^{\text{LJ}} + E^{\text{Torsion}} \quad (4)$$

- Quantized fracture mechanics.** QFM is derived from Griffith's theory based on the assumption of discretized crack propagation through operating the fracture stress from linear elastic fracture stress [6], where the fracture stress in QFM writes:

$$\sigma_F(\mathfrak{L}, \rho) = K_{IC} \sqrt{\frac{1 + \frac{\rho}{2L_0}}{\pi(\mathfrak{L} + \frac{L_0}{2})}} \quad (5)$$

where K_{IC} is the fracture intensity to be fitted for verifications.

Verification from Quantized Fracture Mechanics

The fitted curve from QFM (black dashed lines) well matches MD simulation data as shown in Figure 2. A nonlinear increase in fracture for smaller defects is reported marked in the arrows.

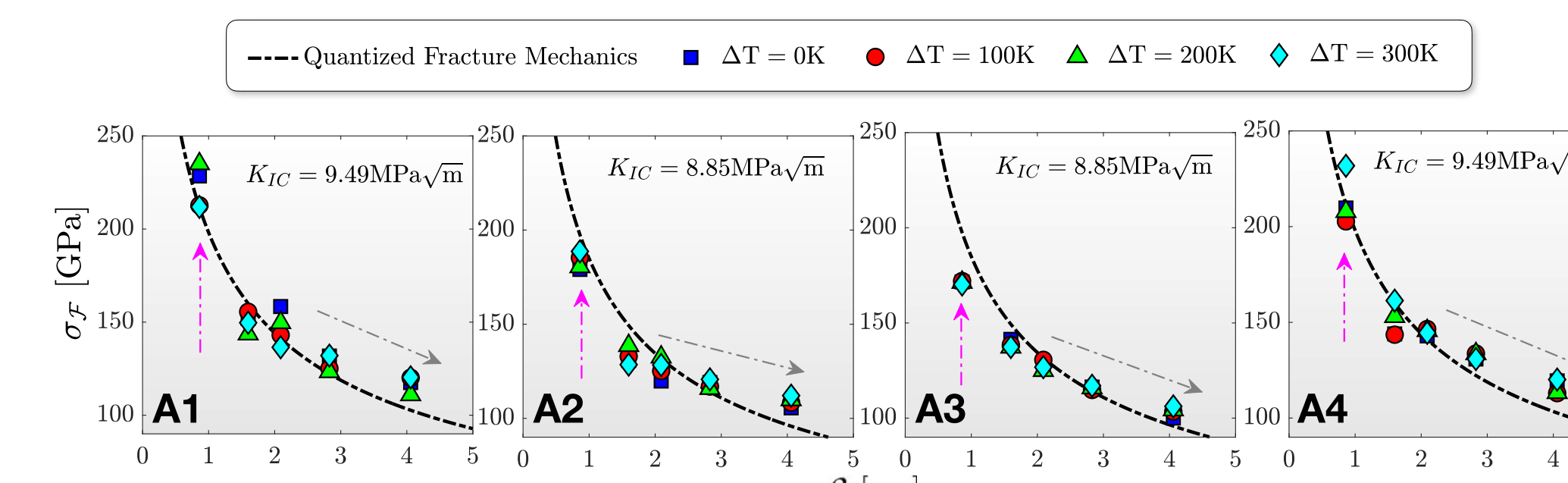


Figure 2. Verification results of the molecular dynamics data fitted with QFM theories.

Anomalous Kinetic Energy Transportation

Considering the case of dynamic failure, the kinetic energy rate should be the difference between the work and elastic energy rate, which is interpreted to drive the dynamic fracture. Herein show an anomalous fracture of kinetic energy transportation in Figure 3.

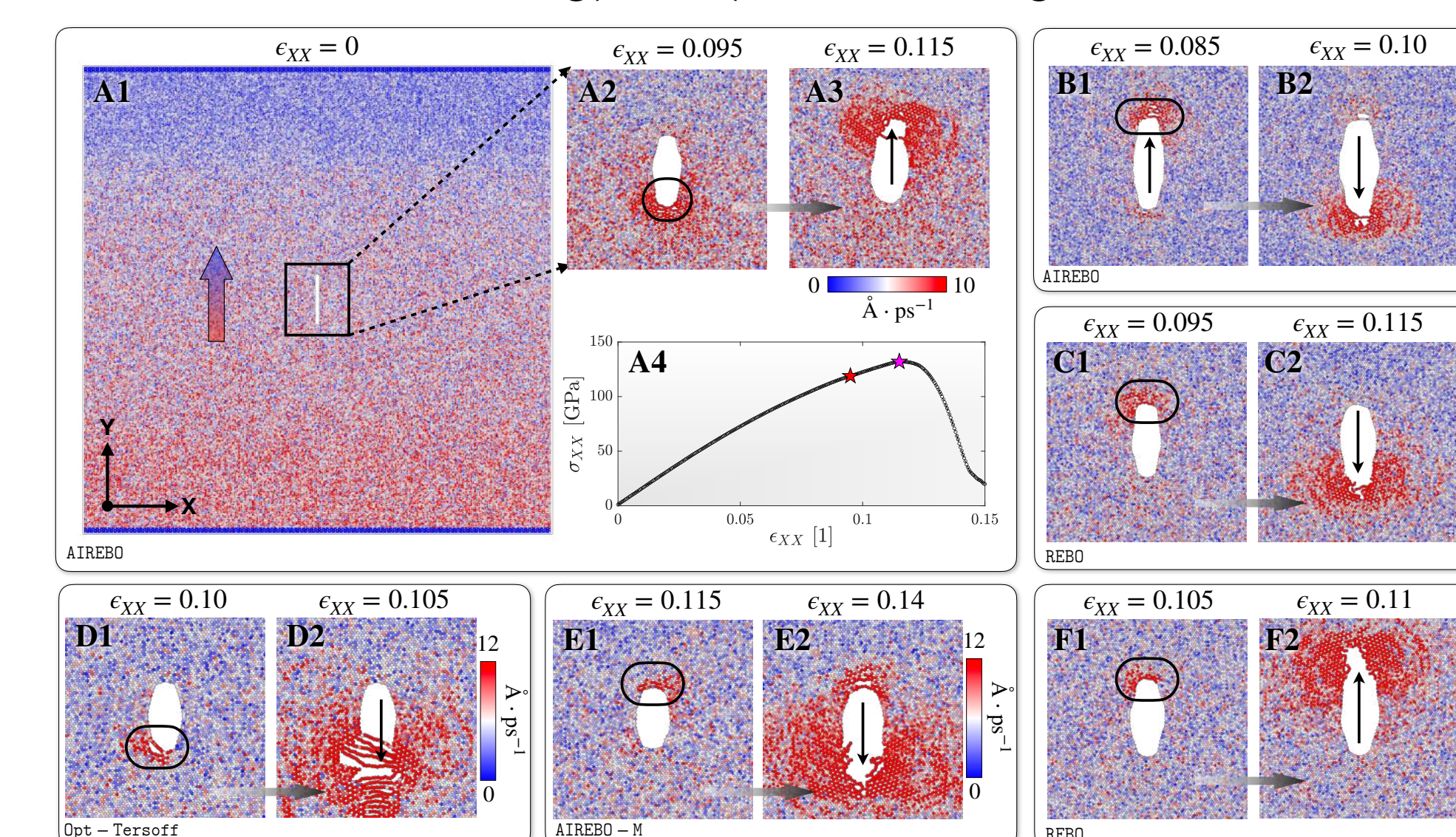


Figure 3. Graphical illustration of the observed "kinetic energy transportation" phenomena during the fractures.

Benchmarking *ab initio* Deep Learning Potentials

Figure 4 shows the results from benchmarking four different MLPs. DUNN with a dropout rate of 0.2 (DUNN v2) surprisingly shows a more accurate energy configuration.

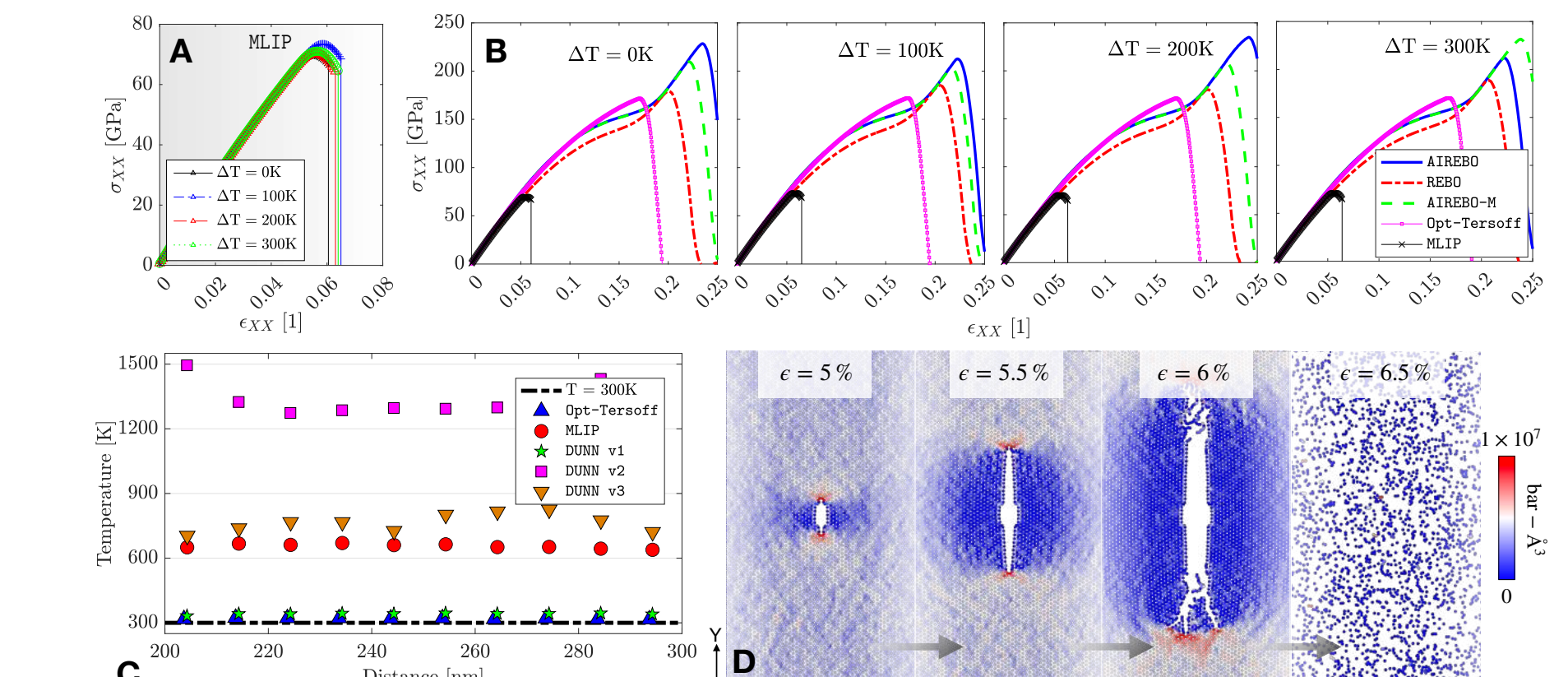


Figure 4. The simulation results for benchmarking the machine learning methods.

Physico-Chemical Perspective of the Nonlinear Mechanics

The transversal bond of a smaller initial crack (closer to a pore) contributes to sharing the loading. This explanation (or guess) is proposed to account for (1) strain-hardening observed for small cracks; (2) nonlinear increasing stress in QFM.

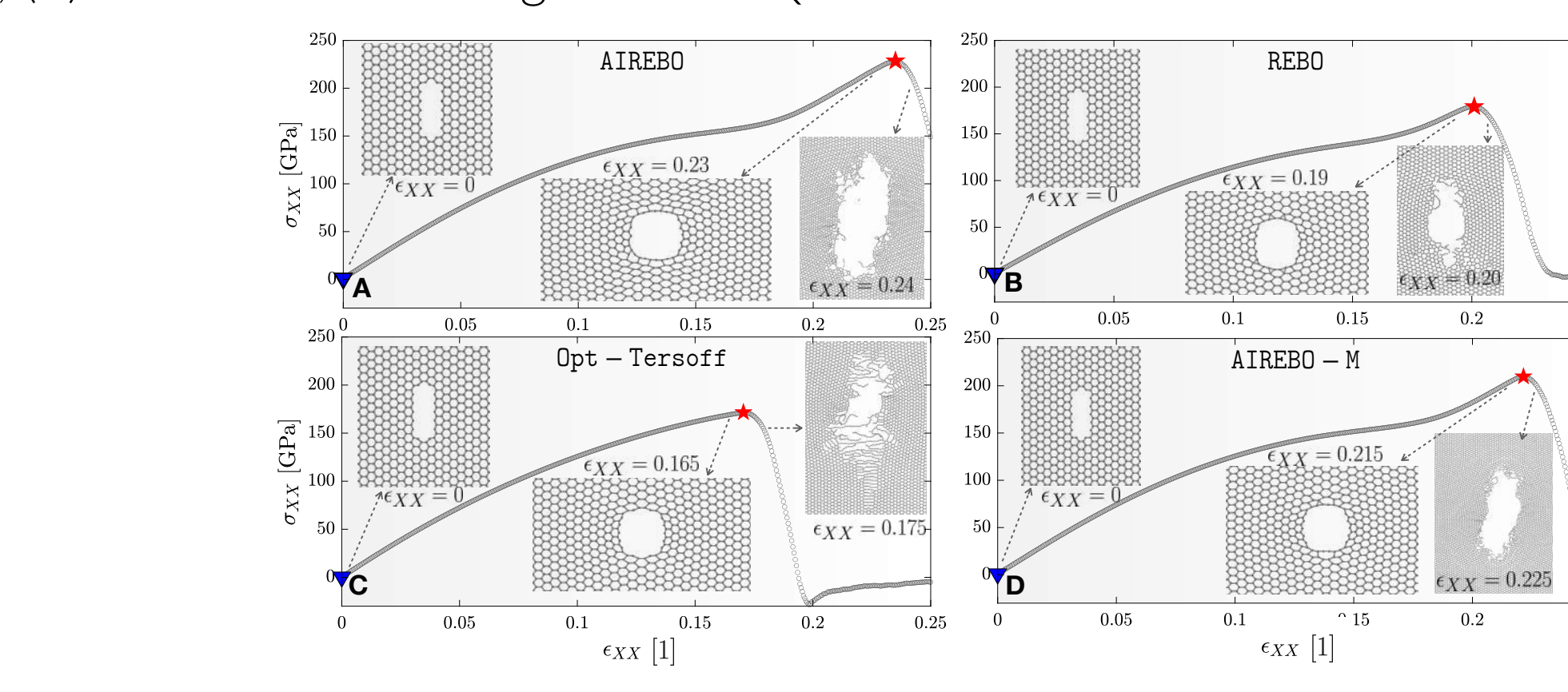


Figure 5. The nonlinear fracture processes employing four different empirical potentials.

Conclusions & Summary

- The stress-strain responses are highly dependent on potentials. The "REBO-based" potentials exhibit strain-hardening effects for a small initial defect.
- The fracture direction is reported to be not related to temperature gradients under $\dot{\epsilon} = 10^9 \text{ s}^{-1}$.
- The fitted fracture intensity K_{IC} matches the literature experimental results.
- An abnormal fracture form is observed for "REBO-based" potentials, where the kinetic energy is transported along with the crack tips before fracture.
- The machine learning interatomic potentials show lower fracture stresses than empirical's.
- The employed deep learning potentials lack the ability to describe post-fracture molecular descriptions, with atoms "exploded" into scattered distributions.

References

- J. Behler and M. Parrinello, *Physical Review Letters*, 98(14), 2007.
- D. W. Brenner, O. A. Shenderova, J. A. Harrison, and et al. *Journal of Physics: Condensed Matter*, 14(4):783–802, 2002.
- L. Lindsay and D. A. Broido, *Physical Review B*, 81(20), 2010.
- I. S. Novikov, K. Gubarev, E. V. Podryabin, and et al. *Machine Learning: Science and Technology*, 2(2):025002, 2021.
- T. C. O'Connor, J. Andzelin, and M. O. Robbins. *The Journal of Chemical Physics*, 142(2):024903, 2015.
- N. M. Pugno and R. S. Ruoff. *Philosophical Magazine*, 84(27):2829–2845, 2004.
- S. J. Stuart, A. B. Tutein, and Judith A. Harrison. *The Journal of Chemical Physics*, 112(14):6472–6486, 2000.
- M. Wen and E. B. Tadmor. *npj Computational Materials*, 6(1), 2020.